*Brazilian Journal of Biometrics*, **43**, 1-22 (2025)
doi:10.28951/bjb.v43i4.776


ARTICLE

# A latent gaussian joint modelling of multivariate longitudinal and mixture cure outcomes with application to aortic valve replacement surgery data[1]

Aniefiok Henry Ekong*[1], Olaniyi Matthew Olayiwola[1], Abayomi Ganiyu Dawodu[1] and Ademola Idowu Osinuga[2]

[1]Department of Statistics, Federal University of Agriculture Abeokuta, Abeokuta, Ogun State, Nigeria.
[2]Department of Mathematics, Federal University of Agriculture Abeokuta, Abeokuta, Ogun State, Nigeria.
*Corresponding author. Email: anieekong@outlook.com;

(Received: October 01, 2024; Revised: February 21, 2025; Accepted: April 14, 2025; Published: September 08, 2025)

**Abstract**

This study examined the effects of different association structures and multivariate longitudinal trajectories, including linear, quadratic and spline functions, on the estimation of time to event and cure proportion under the latent Gaussian model approach with application aortic valve replacement surgery data. The Bayesian framework assumed inverse-Wishart prior distribution for the covariance matrix of the random effects and Gaussian priors for the joint model fixed effects, while the penalised complexity prior was assumed for the Weibull shape parameters of the baseline hazard function. Posterior distributions were evaluated using Integrated Laplace approximation. The modelling approach was applied to aortic valve replacement surgery data to assess the effects of covariates on three longitudinal biomakers on risk of death as well as prediction of cure proportion. Spline trajectories for the multivariate longitudinal biomakers with current slope association was the best fit for the data. The full conditional distribution of latent incidence variable predicted a cure proportion of 36.33% and type of treatment valve with gender of patients were significant in the proportion of cure, risk of death and longitudinal outcomes. The probability of cure depended on the type of implanted aortic prosthesis and gender of patients.

**Keywords**: Survival proportions; Association structure; Laplace approximation; Shared random effect; Nonlinear trajectory; Aortic valve.

## 1. Introduction

Many experiments and trials give rise to opportunity for the collection of different types of datasets at the same time, for example longitudinal and survival datasets. These types of datasets are usually analyzed separately. However, since the two datasets are collected from the same individuals simultaneously, analyzing them separately can overlook latent

association of the two components that could shed better light to the subject of inquiry. Consequently, conclusions may be biased and insufficient as a result of measurement error and missing data. Joint modelling has become a pervasive approach in analyzing these two datasets as a way of remedying the separate analysis (See Tsiatis & Davidian, 2004). Joint modelling has been used in medical and health studies, engineering, finances etc. For example, Oliveira *et al.*, (2024) applied joint modelling to assess the effect of serum chloride and main Strong Ion Difference (mSID) on the survival of severely ill COVID-19 patients. Hickey *et al.*, (2018a) gave a comprehensive review of literatures for implementation of joint models involving more than a single event time per subject. They considered the distributional and modelling assumptions, including the association structure, estimation approaches, software implementations, and clinical applications. Alsefri *et al.*, (2020) gave a review of developments in Bayesian joint models covering articles published up to July 2019.

Classical survival analysis models such as the Cox proportional hazard (PH) model (Cox, 1972) and the accelerated failure time (AFT) (Kalbfleisch & Prentice, 2002) model are based on the assumption that given enough follow up time, every subject will eventually experience the event of interest or censored. In some real situations, there are cases in which some individuals will never experience the event of interest, even if the follow-up is indefinite, or in the case of HIV/AIDS trials, with the availability of improving antiretroviral drugs, it is safe to say that some patients will die of old age or due to other reasons linked with the biological process of ageing. This kind of patient may never experience the event of interest of the HIV/AIDS even if followed up indefinitely. Classical survival models are not-well suited to take into consideration this case of long-term survivors or cured subjects (Martins *et al.*, 2017).

In the case of possibility of cured subjects, the population is assumed to be made up of two groups of subjects: the susceptible, who will one day experience the event of interest, and the cured, who may not experience the event of interest during the follow-up period. Cancer trials are also cases where there is a strong rationale for the existence of cured subjects because if the treatment is successful, the original cancer is removed and the subject will not experience recurrence of the disease. This is particularly true for patients in early cancer stages (Peng & Taylor, 2014). Cure models are particularly appropriate in cancer trials where there is scientific interest in factors associated with the probability of cure and factors associated with the time to recurrence for non-cured individuals.

Joint modelling with multivariate longitudinal outcome with different survival model extensions abound in literature both in frequentist and Bayesian approaches. In frequentist approach, the common estimation method is the expectation-maximization (EM) algorithm and its extensions. For example, Hickey *et al.*, (2018b) introduced Monte Carlo Expectation-Maximization (MCEM) algorithm for estimation of joint model of a multivariate linear mixed sub-model for the longitudinal outcomes and a Cox proportional hazards regression model with time-varying covariates. The algorithm is implemented in their R package joineRML. The association between models is captured through a zero-mean multivariate latent Gaussian process. They suggested that the use of approximate methods for the numerical integration or data reduction methods for large volume of data could be employed in cases their algorithm did not cover. Philipson *et al.*, (2020) proposed the Quasi-Monte Carlo (QMC) methods using quasi-random sequences, instead of pseudo-

random samples for use in the joint modelling of time-to-event and multivariate longitudinal data. The QMC integration framework extends the MCEM approaches using ordinary and antithetic variates in order to increase the convergence speed with nodes that are scattered more uniformly. Murray & Philipson (2022) introduced an approximate EM algorithm for multivariate joint models with linear mixed model for longitudinal process that ameliorates the issue of dimensionality of many classic approaches. Li *et al.*, (2021) proposed a flexible joint model framework that models the multiple biomarkers with a shared latent reduced rank longitudinal principal component model and correlates the latent process to the event time by the Cox model for dynamic prediction of the event time using EM algorithm for parameter estimation.

Bayesian approach has seen more of Markov chain Monte Carlo (MCMC) for parameter estimation, for example, Chen *et al.*, (2004) presented multiple longitudinal markers as well as a cure structure for the survival component based on the promotion time cure rate model with MCMC Gibbs sampling. Chi & Ibrahim (2007) used MCMC adaptive rejection algorithm and an extra Metropolis step was used for parameter estimation in joint modelling of multivariate longitudinal component and cure survival component. He & Luo (2016) employed MCMC in their shared random effects joint model of a multilevel item response theory model for the multiple longitudinal outcomes, and a Cox's proportional hazard model with piecewise constant baseline hazards for the event time data. Alafchi *et al.*, (2021) proposed a two-stage base model for joint modelling of multivariate longitudinal and multistate process. Maximum likelihood estimation was used for fixed effects coefficients in longitudinal and multistate model and empirical Bayes methods for random effects coefficients in longitudinal. Medina-Olivares *et al.*, (2023a) proposed a joint model for bivariate endogenous time-varying covariates and discrete survival data using integrated nested Laplace approximation (INLA) for parameter estimation.

Many studies in the literature report the computational constraint of Markov chain Monte Carlo (MCMC) technique in joint modelling, and they have been shown to be limited to relatively small samples and model specifications, as well as have slow convergence properties (Rustand *et al.*, 2024a). The approximate Bayesian approach, INLA, introduced by Rue *et al.*, (2009) has begun to gain usage for joint modelling as an alternative to MCMC with the Rue *et al.*, (2009) discussing the advantages of INLA over MCMC. We refer to Mayer *et al.*, (2019), van Niekerk *et al.*, (2021), Medina-Olivares *et al.*, (2023b), Rustand *et al.*, (2023), Rustand *et al.*, (2024a), Rustand *et al.*, (2024b), Alvares *et al.*, (2024) and Ekong *et al.*, (2025) for more instances of INLA's applicability and suitability. Lázaro *et al.*, (2020) presented implementation INLA in general mixture cure survival model with covariate information for the latency and the incidence model within a general scenario with censored and non-censored information. van Niekerk *et al.*, (2019) showed that a joint model with a linear bivariate Gaussian association structure is a latent Gaussian model (LGM) and thus can be implemented using most existing packages for LGMs especially R-INLA and van Niekerk *et al.*, (2021) proposed a fully non-parametric spline component to competing risk joint model with nonlinear longitudinal trajectories to capture non-linear behaviour over time in the form of a random walk order two model. Rustand *et al.*, (2024a) presented joint models of multivariate longitudinal and survival data using integrated nested Laplace approximations algorithm implemented in the R package R-INLA. They compared the INLA method to existing alternatives (MCMC and MCEM) via simulations applied to five longitudinal markers and included competing risks

of death and transplantation in application to clinical trial on primary biliary cholangitis.

This study builds on the presentation of Rustand *et al.*, (2024a) and extends the joint modelling of Ekong *et al.*, (2025) to multivariate longitudinal outcomes to cure survival outcomes, with shared random effect. We examine the effects of different association structures and different functions for the longitudinal trajectories which includes linear, quadratic and spline functions, on the estimation of time to event as well as cure proportion. We considered application to real dataset of aortic valve replacement surgery from an observational study by Lim *et al.*, (2008), on detecting effects of different heart valves, differing on type of tissue, implanted in the aortic position. Our interest in this study included the trajectories of the multivariate longitudinal measurements and the possibility of cure as a result of censoring, lost at follow-up or non-occurrence of the failure event at the end of follow-up or study period. The model will seek to address the questions of what proportion of patients that were cured by the effect of the treatment?

## 2. Materials and Methods

Given sample observation of the $p$-th longitudinal variable as $y_{imp}$, ($p$ = 1, …, $P$) on the $i$-th patient ($i$ = 1, …, $N_L$) at the $m$-th time point, let $T_{im}$ be the observed event time for the $i$-th patient at the $m$-th time point, which may be right censored. The event indicator is given as $\delta_i$ = 1 if event is observed and $\delta_i$ = 0 if censored and $Z_i$ then is the latent variable classifying the patient as cured or not at the end of the follow-up. We observe that any patient with survival time observation at a particular point in time is classified to the population of uncured patients.

The observed data for the $i$-th patient without any covariate is $\boldsymbol{D}_i = \{ \boldsymbol{y}_{imp} , T_{im} , \delta_i , Z_i \}$. The $\boldsymbol{D}_i$ 's are assumed to be independent across patients, reflecting the belief that the disease process evolves independently for each patient. We also assume that $T_{im}$ and $\boldsymbol{y}_{imp}$ are conditionally independent given some covariates of interest and a set of unobserved subject-level random effects. One problem associated with the cure model is identifiability and this arises due to the lack of information at the end of the follow-up period, since a significant proportion of patients are censored before the end of the follow-up period. Consequently, it can be difficult to differentiate models with high incidence of susceptible and long tails of the failure time process from low incidence of susceptible and short tails of the failure time process. Analysing survival cure model with longitudinal data simultaneously helps reduce the uncertainty about the tail of the failure time distribution for susceptible (Yu *et al.*, 2008).

### 2.1 Longitudinal model component

Given $p$-th longitudinal variable observation $y_{imp}$ and assuming that for a marginal generalized linear model, the population is from some probability model with density $f(\boldsymbol{Y}|\boldsymbol{X};\boldsymbol{\beta};\boldsymbol{U})$. We also assume that the longitudinal outcomes $y_{imp}$, are conditionally independent and follow a well-defined distribution, $G$, with some density function $g$, linear predictor $\eta^L$ and hyperparameters $\boldsymbol{\theta}^L$, hence a structured additive model for the longitudinal component is given as follows:

$$g^{-1}\{E(y_{imp}|\boldsymbol{X},\boldsymbol{\beta},\boldsymbol{U})\} = \boldsymbol{\eta}^L = \boldsymbol{\beta}_0 + \boldsymbol{\beta}\boldsymbol{X} + \sum_{i=1}^{N_L}\sum_{p=1}^{P} f_p(\boldsymbol{u}_{ip}) + \boldsymbol{b}_i\boldsymbol{u}_i + \boldsymbol{\epsilon}, \qquad (1)$$

where $f_p(\boldsymbol{u}_{ip})$ is the $p$-th latent random effect of covariate $\boldsymbol{u}_{ip}$ for $i$-th patient. We shall

look at both a quadratic and spline function for the latent random effect to account for possible nonlinear trajectories in the longitudinal variables. $\boldsymbol{\beta}$ represent the fixed effects of the covariates $\boldsymbol{X}$, $\epsilon$ is the unstructured random effects. $\boldsymbol{b}_i$ is the vector of random effects of intercept and slope, where $\boldsymbol{\beta}_0$ plus $\boldsymbol{b}_{ip}$ gives the combined effect of the intercept and random intercepts terms specifying that the event depends on the patient-specific level of the longitudinal profile at time $t = 0$. The random effects $\boldsymbol{b}_i$ measure the intra-and-inter-variable correlation between the repeated measurements of an individual (Rustand *et al.*, 2024a) and are assumed to be multivariate normally distributed:

$$\boldsymbol{b}_i = \begin{bmatrix} b_{i1} \\ \vdots \\ b_{ip} \end{bmatrix} \sim MVN\left( \begin{bmatrix} \mathbf{0} \\ \vdots \\ \mathbf{0} \end{bmatrix}, \quad \begin{bmatrix} \boldsymbol{\Sigma}_{b_{i1}} & \cdots & \boldsymbol{\Sigma}_{b_{i1}b_{ip}} \\ \vdots & \ddots & \vdots \\ \boldsymbol{\Sigma}_{b_{i1}b_{ip}} & \cdots & \boldsymbol{\Sigma}_{b_{i1}} \end{bmatrix} \right).$$

## 2.2 Cure survival model component

Given the observed event time $T_{im}$, let $Z_i$ be a cure random variable defined as $Z_i = 0$ if that patient is susceptible for experiencing the event of interest, and $Z_i = 1$ if the patient is cured. Cure and uncured probabilities are $P(Z_i = 1) = \pi$ and $P(Z_i = 0) = 1 - \pi$, respectively. The survival functions for patients in the cured and uncured population, $S_c(t)$ and $S_u(t)$, $t > 0$, respectively, are

$$S_u(t) = P(T_{im} > t \,|Z_i = 0)$$

$$S_c(t) = P(T_{im} > t \,|Z_i = 1) = 1.$$

The general survival function for $T_{im}$ can be expressed in terms of a mixture of both cured and uncured populations in the form

$$S(t) = P(T_{im} > t) = \pi + (1 - \pi)S_u(t). \tag{2}$$

Cure fraction $\pi$ is also known as the incidence model and event time $T_{im}$ in the uncured population is also referred to as the latency model (Peng and Taylor, 2014).

### *2.2.1 Covariates in the incidence model*

Note that for a patient who has experienced the event ($\delta_i = 1$), we know $Z_i = 1$, but for a censored patient ($\delta_i = 0$), we do not observed $Z_i$, hence, the effect of a baseline covariate vector $\boldsymbol{x}_1$ on the cure proportion is typically modelled by means of a logistic link function expressed as

$$\text{logit}[\pi\,(\boldsymbol{\beta}_1)] = \boldsymbol{\beta}_1'\boldsymbol{x}_1 \equiv \pi(\beta_1) = \frac{\exp\{\boldsymbol{\beta}_1'\boldsymbol{x}_1\}}{1 + \exp\{\boldsymbol{\beta}_1'\boldsymbol{x}_1\}}, \tag{3}$$

where $\boldsymbol{\beta}_1$ is the vector of regression coefficients associated to $\boldsymbol{x}_1$ and $\pi$ is the cure proportion.

### *2.2.2 Covariates in the latency model*

For patients with $Z_i = 1$, the time to event is assumed to follow a parametric distribution. The Cox proportional hazards model is usually formulated in terms of the hazard function for the event time as

$$h_u(t \,|h_{u0}, \boldsymbol{\beta}_2) = \lim_{\Delta t \to \infty} \frac{P(t \leq T_{im} < t + \Delta t \,|T \geq t)}{\Delta t} = h_{u0}(t)\exp\{\boldsymbol{\beta}_2'\boldsymbol{x}_2\}, \tag{4}$$

where $h_{u0}(t)$ is the baseline hazard function that determines the shape of the hazard function. Model (4) can also be presented in terms of the survival function of $T_{im}$ as

$$S_u(t|S_{u0}, \boldsymbol{\beta}_2) = [S_{u0}(t)]^{exp\{\boldsymbol{\beta}_2' \boldsymbol{x}_2\}}, \tag{5}$$

where $S_{u0}(t) = \exp\left\{-\int_0^t h_{u0}(s)\mathrm{d}s\right\}$ represents the survival baseline function and some hyperparameter $\theta^S$.

## 2.3 Joint Model of Multivariate Longitudinal and Cure Survival Outcomes as LGMs

The modelling approach assumes a logistic distribution for the probability of cure in the incidence model in (3) and the Cox proportional hazard (4) for the survival time with a Weibull baseline hazard function $h_{u0}(t|\lambda,\ \alpha) = \lambda\alpha t^{\alpha-1}$ with $\lambda$ and $\alpha$ as the scale and shape parameters respectively. $\gamma_p$ is the association parameter estimating the strength of association between the survival and the *p*th longitudinal component, thus we define

$$h_i(s) = h_{u0}(s)\eta_i^S(s)\left(\exp\left\{-\int_0^t h_i(u)\mathrm{du}\right\} + \mathrm{logit}[\pi\,]\right). \tag{6}$$

The linear predictors of the joint model becomes

$$\eta_i^{L,J}(t) = \boldsymbol{\eta}_i^L(t)$$

$$\eta_i^{S,J}(s) = \eta_i^S(s) + \gamma_p\left(\boldsymbol{\eta}_i^L(s)\right). \tag{7}$$

Here $\gamma_p$ as a smooth function facilitates the joint estimation of the models associating the longitudinal trajectories and mixture cure process using the entire longitudinal predictors as shared random effect where each random effect's individual deviation is associated to an association parameter in the survival latency component. We consider in this study three association structures as defined in INLAjoint (Rustand *et al.*, 2024b) package, extending the univariate longitudinal case studied in Ekong *et al.*, (2025) to include the associations through sharing of the current value of the linear predictors (CV), association through sharing current slope (CS) and association through sharing the individual deviation from the mean at time *t* as defined by the random effects (SRE). More details of the different association structures can be found in Rustand *et al.*, (2024b).

### *2.3.1 Likelihood function of Joint Model*

The likelihood of the longitudinal outcomes given the parameters $\boldsymbol{\beta}_0, \boldsymbol{\beta}, \theta^L, \boldsymbol{\eta}^L, f_p(\cdot), \boldsymbol{b}_i$ and $\boldsymbol{\epsilon}$ can be given as

$$\mathcal{L}^L(\boldsymbol{y}|\boldsymbol{\eta}^L) = \prod_{p=1}^{P}\prod_{i=1}^{N_L} g\left(y_{imp}\middle|\boldsymbol{\eta}_i^L(t)\right). \tag{8}$$

Given survival observations $\boldsymbol{d} = \{T_{im}\ ,\ \delta_{im}\ ,\ z_{im}\}$ and parameter vector $\boldsymbol{R} = \left(\boldsymbol{\beta}_1, \boldsymbol{\beta}_2, \alpha, \lambda, \boldsymbol{\eta}^S, \theta^S, \gamma_p\right)$, the likelihood for the mixture cure survival becomes

$$\mathcal{L}^S(\boldsymbol{d}|\boldsymbol{R}) = \prod_{i=1}^{N}\mathcal{L}_i(\boldsymbol{R}|d) = \prod_{i=1}^{N}\eta_i^S\boldsymbol{R}^{z_i}\left(1-\eta_i^S\boldsymbol{R}\right)^{1-z_i}h_{iu}(t_i|\boldsymbol{R})^{\delta_i(1-z_i)}S_{iu}(t_i|\boldsymbol{R})^{1-z_i}. \tag{9}$$

The complete likelihood becomes

$$p(\boldsymbol{D}_i|\boldsymbol{\chi}_i,\boldsymbol{\theta}) = \int_{\boldsymbol{b}_i}\left[\prod_{i=1}^{N}\mathcal{L}_i(\boldsymbol{R}|d)\prod_{p=1}^{P}\prod_{i=1}^{N_L} g\left(y_{imp}\middle|\boldsymbol{\eta}_i^L(t)\right)p(\boldsymbol{b}_i)\right]d\boldsymbol{b}_i, \tag{10}$$

where we define the latent field $\boldsymbol{\chi} = (\boldsymbol{\beta}, \boldsymbol{\beta}_1, \boldsymbol{\beta}_2, \boldsymbol{\eta}^S, \boldsymbol{\eta}^L, f_p(\cdot), \boldsymbol{b}_i, \lambda, \boldsymbol{\epsilon})$ and a vector of hyperparameters $\boldsymbol{\theta} = \left(\theta^L, \theta^S, \alpha, \tau^{-1}, \gamma_p\right)$. Under the assumption that the Gaussian field is conditionally independent, i.e., the latent field is a Gauss Markov Random Field (GMRF) (Rue & Held, 2005; Blangiardo & Cameletti 2015), the likelihood function in equation (10) provides the distribution of the *pm* observations, where each data point $\boldsymbol{D}_i$ is associated with only one element in the latent field $\boldsymbol{\chi}_i$. This suggests that $\boldsymbol{D}_i$ and $\boldsymbol{\chi}_i$ have the same dimension and that the parameters are constant.

The main task is to present equation (10) as LGMs by showing its specific hierarchical structure. The first level of the hierarchy involves presenting the likelihood function given the latent field $\boldsymbol{\chi}$ and the vector of hyperparameters $\boldsymbol{\theta}$ as shown in equation (10). The next level of the hierarchy involves the conditional distribution of the latent field $\boldsymbol{\chi}$ which is assumed to have a multivariate Gaussian prior with zero mean, such that it forms a Gaussian Markov random field with sparse precision matrix matrix $\boldsymbol{Q}(\boldsymbol{\theta}_2)$, i.e. $\boldsymbol{\chi}\sim MVN(\boldsymbol{0}, \boldsymbol{Q}^{-1}(\boldsymbol{\theta}_2))$, this is given as

$$p(\boldsymbol{\chi}|\boldsymbol{\theta}) = (2\pi)^{pm}|\boldsymbol{Q}(\boldsymbol{\theta}_2)|^{-\frac{1}{2}}\exp\left(-\frac{1}{2}\boldsymbol{\chi}'\boldsymbol{Q}(\boldsymbol{\theta}_2)\boldsymbol{\chi}\right). \tag{11}$$

Then at the final level of the hierarchy, a prior on the hyperparameter vector $p(\boldsymbol{\theta})$ can then be formulated for the set of hyperparameters $\boldsymbol{\theta} = (\boldsymbol{\theta}_1, \boldsymbol{\theta}_2)$, which could be non-normal. This enables us to assume normal prior for the vector of fixed effects for the *p*th longitudinal variable as $\boldsymbol{\beta}_p\sim N(\boldsymbol{0}, \tau_{\boldsymbol{\beta}_p}\boldsymbol{I})$, where $\boldsymbol{\beta}_p \in \boldsymbol{\chi}$ and $\tau_{\boldsymbol{\beta}_p} \in \boldsymbol{\theta}$. To complete the model specification, we assume the inverse-Wishart prior distribution for the covariance matrix of the random effects and Gaussian priors for the fixed effects, while the penalised complexity prior PC(5) is assumed for the Weibull shape parameters of the baseline hazard function.

From this hierarchical Bayesian formulation the joint posterior distribution is then given as:

$$\begin{aligned} p(\boldsymbol{\chi},\boldsymbol{\theta}|\boldsymbol{D}) &\propto p(\boldsymbol{\theta})p(\boldsymbol{\chi}|\boldsymbol{\theta})\prod_{\boldsymbol{i}} p(\boldsymbol{D}_i|\boldsymbol{\chi},\boldsymbol{\theta}), \\ &\propto p(\boldsymbol{\theta})|\boldsymbol{Q}(\boldsymbol{\theta}_2)|^{\frac{1}{2}}\exp\left(-\frac{1}{2}\boldsymbol{\chi}'\boldsymbol{Q}(\boldsymbol{\theta}_2)\boldsymbol{\chi} + \sum_{\boldsymbol{i=1}}^{\boldsymbol{n}}\log(\boldsymbol{D}_i|\boldsymbol{\chi}_i,\boldsymbol{\theta})\right). \end{aligned} \tag{12}$$

Within this framework the joint posterior density (10) and subsequently the marginal posterior densities, $p(\boldsymbol{\chi}_i|\boldsymbol{D})$; $i = 1, \ldots, n$ and $p(\boldsymbol{\theta}|\boldsymbol{D})$ can be efficiently and accurately calculated using the integrated Laplace approximation (INLA) methodology developed by Rue *et al.*, (2009). The marginal posterior densities becomes

$$p(\boldsymbol{\chi}_i|\boldsymbol{D}) = \int p(\boldsymbol{\chi}_i,\boldsymbol{\theta}|\boldsymbol{D})\,d\boldsymbol{\theta} = \int p(\boldsymbol{\chi}_i,\boldsymbol{\theta}|\boldsymbol{D})p(\boldsymbol{\theta}|\boldsymbol{D})\,d\boldsymbol{\theta}, \tag{13}$$

and

$$p(\theta_i|\boldsymbol{D}) = \int p(\boldsymbol{\theta}|\boldsymbol{D})\,d\boldsymbol{\theta}_{-\boldsymbol{i}}, \tag{14}$$

where $d\boldsymbol{\theta}_{-i}$ denotes all the elements in $\boldsymbol{\theta}$ except the $i$-th element. INLA computes these marginal posteriors by computing the marginal posterior distributions of the hyper-parameters $p(\boldsymbol{\theta}_i|\boldsymbol{D})$, and then the conditional posterior distribution $p(\boldsymbol{\chi}_i|\boldsymbol{\theta},\boldsymbol{D})$, for use in approximating the marginal posterior of the parameters $p(\boldsymbol{\chi}_i|\boldsymbol{D})$, for which a mention of the procedure is given in the next section.

### 2.3.2 Posterior Estimation using Integrated Laplace Approximation

To obtain the posterior distribution of the model parameters under Bayesian framework, by Bayes' theorem, the conditional posterior distribution

$$p(\boldsymbol{\theta}_i,\boldsymbol{\chi}_i|\boldsymbol{D}_i)=\frac{p(\boldsymbol{D}_i|\boldsymbol{\theta}_i,\boldsymbol{\chi}_i)p(\boldsymbol{\theta}_i,\boldsymbol{\chi}_i)}{p(\boldsymbol{D}_i)}\propto p(\boldsymbol{D}_i|\boldsymbol{\theta}_i,\boldsymbol{\chi}_i)p(\boldsymbol{\chi}_i|\boldsymbol{\theta}_i)p(\boldsymbol{\theta}_i), \tag{15}$$

where $p(\boldsymbol{\chi}_i|\boldsymbol{\theta}_i)$ and $p(\boldsymbol{\theta}_i)$ are prior distributions and the focus is on approximating the multidimensional integral from the marginal likelihood $p(\boldsymbol{D}_i|\boldsymbol{\theta}_i,\boldsymbol{\chi}_i)$ and approximation technique of INLA has been shown to provide exact approximations to the posterior estimates at faster rates than sampling-based methods such as Markov Chain Monte Carlo (MCMC) especially for complex and hierarchical models (see Rustand *et al.*, (2024a)).

The posteriors of interest are quantitatively approximated by INLA using the Laplace transformation (Rue *et al.*, 2009) for which we consider here using a second-order Taylor series expansion for the integral of the density function $p(\boldsymbol{\chi})$ by taking the form of (Blangiardo & Cameletti, 2015)

$$\int_{-\infty}^{\infty} p(\boldsymbol{\chi})\,d\boldsymbol{\chi}=\int_{-\infty}^{\infty}\exp(\log p(\boldsymbol{\chi}))\,d\boldsymbol{\chi}=\int_{-\infty}^{\infty}\exp\big(g(\boldsymbol{\chi})\big)\,d\boldsymbol{\chi}. \tag{16}$$

Since for unimodal functions the integral value is mainly determined by the behaviour around the mode of $g(\boldsymbol{\chi})$, a second-order Taylor approximation of $g(\boldsymbol{\chi})$ can be substituted for $g(\boldsymbol{\chi})$ to calculate an approximate value of the integral.

Let $\boldsymbol{\chi}^*$ be the global maximum of $\boldsymbol{\chi}$ which is defined as

$$\boldsymbol{\chi}^*=\text{argmax}_{\boldsymbol{\chi}}\,g(\boldsymbol{\chi}),$$

then

$$\left.\frac{\partial g(\boldsymbol{\chi})}{\partial\boldsymbol{\chi}}\right|_{\boldsymbol{\chi}=\boldsymbol{\chi}^*}=0,$$

for $g(\boldsymbol{\chi})$ to be approximated as

$$g(\boldsymbol{\chi})\approx g(\boldsymbol{\chi}^*)+0.5(\boldsymbol{\chi}-\boldsymbol{\chi}^*)'\mathbf{H}g(\boldsymbol{\chi}^*)(\boldsymbol{\chi}-\boldsymbol{\chi}^*),$$

where $\mathbf{H}g(\boldsymbol{\chi}^*)$ is the Hessian of $g(\boldsymbol{\chi}^*)$, and equation (10) can be written as

$$\begin{aligned}\int_{-\infty}^{\infty} p(\boldsymbol{\chi})\,d\boldsymbol{\chi}&=\int_{-\infty}^{\infty}\exp\big(g(\boldsymbol{\chi}^*)+0.5(\boldsymbol{\chi}-\boldsymbol{\chi}^*)'\mathbf{H}g(\boldsymbol{\chi}^*)(\boldsymbol{\chi}-\boldsymbol{\chi}^*)\big)\,d\boldsymbol{\chi}\\&=\exp\big(g(\boldsymbol{\chi}^*)\big)\int_{-\infty}^{\infty}\exp\big(0.5(\boldsymbol{\chi}-\boldsymbol{\chi}^*)'\mathbf{H}g(\boldsymbol{\chi}^*)(\boldsymbol{\chi}-\boldsymbol{\chi}^*)\big)\,d\boldsymbol{\chi}\\&=\exp\big(g(\boldsymbol{\chi}^*)\big)\int_{-\infty}^{\infty}\exp\big(-0.5(\boldsymbol{\chi}-\boldsymbol{\chi}^*)'\{-\mathbf{H}g(\boldsymbol{\chi}^*)\}(\boldsymbol{\chi}-\boldsymbol{\chi}^*)\big)\,d\boldsymbol{\chi}\\&=\exp\big(g(\boldsymbol{\chi}^*)\big)\,(2\pi)^{\frac{nm}{2}}|\mathbf{H}g(\boldsymbol{\chi}^*)|^{-\frac{1}{2}}\times\end{aligned}$$

$$\int_{-\infty}^{\infty} (2\pi)^{-\frac{nm}{2}} |\mathbf{H}g(\boldsymbol{\chi}^*)|^{-\frac{1}{2}} \exp\left(-0.5(\boldsymbol{\chi}-\boldsymbol{\chi}^*)'\{-\mathbf{H}g(\boldsymbol{\chi}^*)\}(\boldsymbol{\chi}-\boldsymbol{\chi}^*)\right) d\boldsymbol{\chi}.$$

The integral is associated with the density of a multivariate Gaussian distribution and putting $-\mathbf{H}g(\boldsymbol{\chi}^*) = \boldsymbol{Q}(\boldsymbol{\chi}^*)$, the precision matrix for the random vector $\boldsymbol{\chi}^*$ yields

$$\int_{-\infty}^{\infty} p(\boldsymbol{\chi})\, d\boldsymbol{\chi} \approx \exp\left(g(\boldsymbol{\chi}^*)\right) (2\pi)^{\frac{nm}{2}} |\mathbf{H}g(\boldsymbol{\chi}^*)|^{-\frac{1}{2}} \times$$

$$\int_{-\infty}^{\infty} (2\pi)^{-\frac{nm}{2}} |\boldsymbol{Q}(\boldsymbol{\chi}^*)|^{-\frac{1}{2}} \exp\left(-0.5(\boldsymbol{\chi}-\boldsymbol{\chi}^*)'\boldsymbol{Q}(\boldsymbol{\chi}^*)(\boldsymbol{\chi}-\boldsymbol{\chi}^*)\right) d\boldsymbol{\chi}$$

$$\approx (2\pi)^{\frac{nm}{2}} |\boldsymbol{Q}(\boldsymbol{\chi}^*)|^{-\frac{1}{2}} \exp\left(g(\boldsymbol{\chi}^*)\right). \tag{17}$$

The conditional posterior distribution of $p(\boldsymbol{\chi}, \boldsymbol{\theta}|\boldsymbol{D})$ is defined from the joint posterior distribution in Equation (9) as

$$p(\boldsymbol{\chi}, \boldsymbol{\theta}|\boldsymbol{D}) \propto p(\boldsymbol{\theta})|\boldsymbol{Q}(\boldsymbol{\theta})|^{\frac{1}{2}} \exp\left(-\frac{1}{2}\boldsymbol{\chi}'\boldsymbol{Q}(\boldsymbol{\theta})\boldsymbol{\chi} + \sum_{i=1}^{n} \log p(\boldsymbol{D}_i|\boldsymbol{\chi}_i, \boldsymbol{\theta})\right),$$

which can be rewritten as, ignoring elements with $\boldsymbol{\chi}$

$$p(\boldsymbol{\chi}|\boldsymbol{\theta}, \boldsymbol{D}) \propto \exp\left(-\frac{1}{2}\boldsymbol{\chi}'\boldsymbol{Q}(\boldsymbol{\theta})\boldsymbol{\chi} + \sum_{i=1}^{n} g_i(\boldsymbol{\chi}_i)\right). \tag{18}$$

#### *2.3.2.1 Gaussian Approximation*

The Gaussian approximation of Equation (18), $p_G(\boldsymbol{\chi}|\boldsymbol{\theta}, \boldsymbol{D})$ is reached by matching the mode and the curvature at the mode of $p(\boldsymbol{\chi}|\boldsymbol{\theta}, \boldsymbol{D})$. The mode is computed iteratively by using a Newton Raphson method. Let $\mu^{(0)}$ be the initial value of the mode, and expand $g_i(\boldsymbol{\chi}_i)$ around $\boldsymbol{\mu}_i^{(0)} = \left(\mu_{i1}^{(0)}, \ldots, \mu_{iN}^{(0)}\right)$ to the second order Taylor expansion,

$$g_i(\boldsymbol{\chi}_i) \approx g_i\left(\boldsymbol{\mu}_i^{(0)}\right) + \boldsymbol{b}_i'\boldsymbol{\chi}_i - \frac{1}{2}\boldsymbol{c}_i'\boldsymbol{\chi}_i'\boldsymbol{\chi}_i, \tag{19}$$

where $\boldsymbol{b}_i$ and $\boldsymbol{c}_i$ depend on $\boldsymbol{\mu}^{(0)}$. Substituting equation (19) into equation (18) yields

$$p_G(\boldsymbol{\chi}|\boldsymbol{\theta}, \boldsymbol{D}) \approx g_i\left(\boldsymbol{\mu}_i^{(0)}\right) \exp\left(-\frac{1}{2}\boldsymbol{\chi}'(\boldsymbol{Q}+\boldsymbol{c})\boldsymbol{\chi} + \boldsymbol{b}'\boldsymbol{\chi}\right)$$

$$\propto \exp\left(-\frac{1}{2}\boldsymbol{\chi}'(\boldsymbol{Q}+\boldsymbol{c})\boldsymbol{\chi} + \boldsymbol{b}'\boldsymbol{\chi}\right).$$

A Gaussian approximation of $p_G(\boldsymbol{\chi}|\boldsymbol{\theta}, \boldsymbol{D})$ is obtained, with the precision matrix $(\boldsymbol{Q} + \text{diag}(\boldsymbol{c}))$ and mode $\boldsymbol{\mu}^{(1)}$, which is the solution of $\left(\boldsymbol{Q} + \text{diag}(\boldsymbol{c})\right)\boldsymbol{\mu}^{(1)} = \boldsymbol{b}$. The process can then be iterated, with $\boldsymbol{\mu}^{(1)}$as the new starting value, until it converges to a Gaussian distribution with, say, mean $\boldsymbol{\mu}^{(j)} \to \boldsymbol{\mu}^{(*)} = \boldsymbol{\chi}^*$ and precision matrix $\boldsymbol{Q}^{(j)} \to \boldsymbol{Q}^{(*)} = \boldsymbol{Q} + \text{diag}(\boldsymbol{c}^*), j = 1,2, \ldots$, where an appropriate convergence criterion must be used.

The resulting approximation will then be (Opitz, 2017):

$$p_G(\boldsymbol{\chi}|\boldsymbol{\theta}, \boldsymbol{D}) \propto \exp\left(-\frac{1}{2}\left(\boldsymbol{\chi} - \boldsymbol{\chi}^*(\boldsymbol{\theta})\right)'\left(\boldsymbol{Q}(\boldsymbol{\theta}) + \text{diag}(\boldsymbol{c})\right)\left(\boldsymbol{\chi} - \boldsymbol{\chi}^*(\boldsymbol{\theta})\right)\right), \tag{20}$$

where $\boldsymbol{c}$ is the second-order term in the Taylor expansion of $\sum_{i=1}^{n} \log p(\boldsymbol{D}_i|\boldsymbol{\chi}_i, \boldsymbol{\theta})$ at modal value $\boldsymbol{\chi}^*(\boldsymbol{\theta})$.

For the marginal posterior conditional distribution $p(\boldsymbol{\chi}_i|\boldsymbol{\theta}, \boldsymbol{D})$ included in the computation of the marginal posterior $p(\boldsymbol{\chi}_i|\boldsymbol{D})$, Rue *et al.*, (2009) discussed three approximations $\tilde{p}(\chi_i|\boldsymbol{\theta}_k, \boldsymbol{D})$

where $\boldsymbol{\theta}_k$ are weighted points to be used in the integration, Gaussian, full Laplace and simplified Laplace approximation. The Gaussian approximation is generally not best if the true density of $p(\boldsymbol{\chi}_i|\boldsymbol{\theta}, \boldsymbol{D})$ is not symmetric, the full Laplace approximation is a correction of Gaussian approximation and accurate but at a very expensive computational cost, the simplified Laplace approximation which is based on the Taylor series expansion of the full Laplace approximation is sufficiently accurate for most applications (Blangiardo & Cameletti, 2015).

If the mean of $\boldsymbol{\chi}$ is $\boldsymbol{\mu}$, the density of $\boldsymbol{\chi}$ is

$$p(\boldsymbol{\chi}) = (2\pi)^{-n/2}|\boldsymbol{Q}|^{1/2} \exp\left[-\frac{1}{2}(\boldsymbol{\chi}-\boldsymbol{\mu})^T\boldsymbol{Q}(\boldsymbol{\chi}-\boldsymbol{\mu})\right]. \quad (21)$$

The sparse matrix $\boldsymbol{Q}$ is factorised as Cholesky triangle product $\boldsymbol{LL}^T$, and only non-zero terms are computed due to the Markov property and $L_{ji} = 0$. Let $\boldsymbol{L}^T\boldsymbol{\chi} = \boldsymbol{r}$ where $\boldsymbol{r} \sim N(\boldsymbol{0}, \boldsymbol{1})$, then we have that $L_{ii}\chi_i = r_i - \sum_{k=i+1}^{n} L_{ki}\chi_k$ for $i = n, \ldots, 1$. Multiplying each side with $\chi_j, j \geq i$ and taking the expectation yields the recursion

$$\Sigma_{ij} = \frac{\partial_{ij}^2}{L_{ii}} - \frac{1}{L_{ii}}\sum_{k=i+1}^{n} L_{ki}\Sigma_{kj} \qquad j \geq i, \quad i = n, \ldots, 1$$

where $\boldsymbol{\Sigma} = \boldsymbol{Q}^{-1}$ is the covariance matrix and $\partial_{ij} = 1$ if $i = j$ and $\partial_{ij} = 0$ otherwise. These recursion results in Gaussian approximations $\tilde{p}_G(\boldsymbol{\chi}|\boldsymbol{\theta}, \boldsymbol{D})$ with mean $\mu_i(\boldsymbol{\theta})$ and marginal variance $\sigma_i^2(\boldsymbol{\theta})$.

# 3. Results and Discussion

## 3.1 Descriptive analyses of the aortic valve replacement surgery data

The aortic valve replacement surgery data is an observational study on detecting effects of different heart valves, differing on type of tissue, implanted in the aortic position carried out by Lim *et al.*, (2008). The data consists of 300 patients who underwent aortic valve replacement from 1991 to 2001 with at least a year of follow-up with a total of 1,273 serial echocardiographic measurements. Patients with two or more procedures were censored from the time point of the second procedure to ensure that they were analysed only once. Demographic, operative, and mortality data were obtained from individual hospital notes, death certificates, and autopsy reports. Details of the dataset can be found in Lim *et al.*, (2008). The version of the aortic valve replacement surgery data (n = 256) used in this study was obtained from the R package joineRML (Hickey *et al.*, 2018b) and for the sake of comparison of results we selected variables used in the analysis in Lim *et al.*, (2008) for our own analysis and they include *hs*, the type of implanted aortic prosthesis: Homograft or Stentless valve; *sex*, gender of patient (0 = Male and 1 = Female); *time*, observed time point, with surgery date as the time origin (years); *fuyrs*, maximum follow up time, with surgery date as the time origin (years); *status*, censoring indicator (1 = died and 0 = lost at follow up); *size*, size of the valve (millimeters); *lv*, preoperative left ventricular ejection fraction (1 = good, 2 = moderate and 3 = poor); *grad*, valve gradient at follow-up visit; *lvmi*, left ventricular mass index (standardised) at follow-up visit; and *ef*, ejection fraction at follow-up visit. The longitudinal multi-variables are *grad, lvmi* and *ef*.

We examine the longitudinal trajectories of the valve gradient (*grad*), left ventricular mass index (*lvmi*) and ejection fraction (*ef*) from the 256 patients who aortic valve replacement surgery at follow-up visits, for three covariates of treatment *hs*, *sex* and *lv* in Figure 1, Figure 2 and Figure 3 respectively. The longitudinal trajectories for three dependent variables do not seem to be linear but nonlinear for both groups of patients who received homograft value and stentless valve for replacement for patients in the *grad* profiles of Figure 1. There seemed to be similar nonlinear trajectories for each of the three longitudinal outcomes for the 123 patients who received the homograft value and the 133 patients who received the stentless valve replacement. The *lvmi* and *ef*

shows polynomial trajectories for which the spline functions can be used to model.

The distribution of patients according to *sex* showed that 183 patients were male and 73 patients were female. Similar patterns of nonlinear longitudinal outcomes profiles are seen for the two groups of male and female patients. Again there seemed to be similar nonlinear trajectories for male and female patients for the three longitudinal outcomes of *grad*, *lvmi* and *ef* as seen in Figure 2. The patients' distribution for the covariate of preoperative left ventricular ejection fraction, *lv*, showed that 147 patients had good preoperative left ventricular ejection fraction, 87 patients had moderate preoperative left ventricular ejection fraction, while 22 had poor preoperative left ventricular ejection fraction. From Figure 3 we see that the three preoperative left ventricular ejection fraction groups had similar longitudinal profiles and particularly those with poor preoperative left ventricular ejection fraction had lowest values of ejection fraction *ef*. It can also be observed that patients with highest *lvmi* values were males with moderate preoperative left ventricular ejection fraction who received homograft valve replacement.

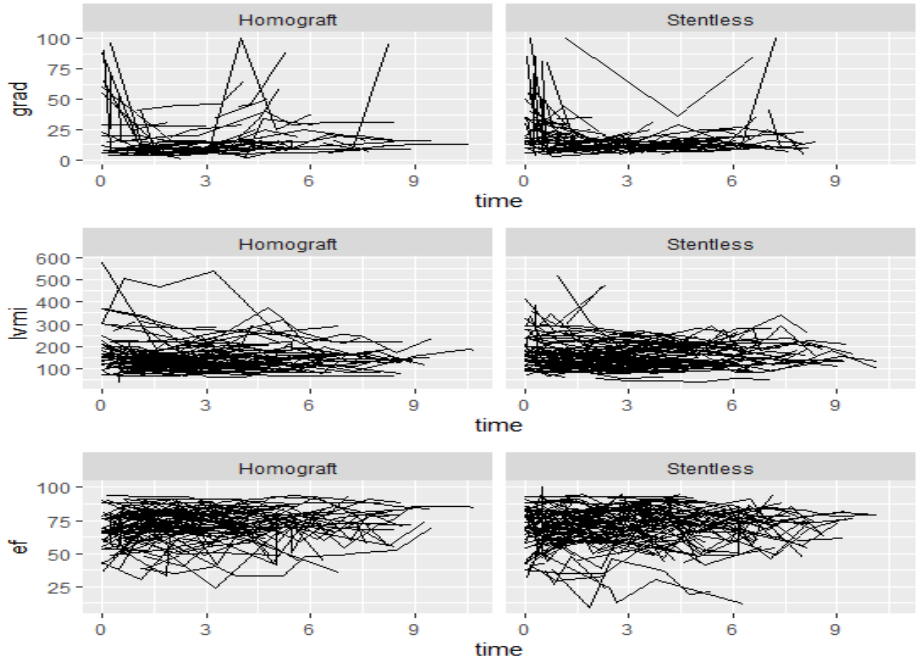


**Figure 1.** The Spaghetti Plot of longitudinal outcomes by treatment covariate *hs.*

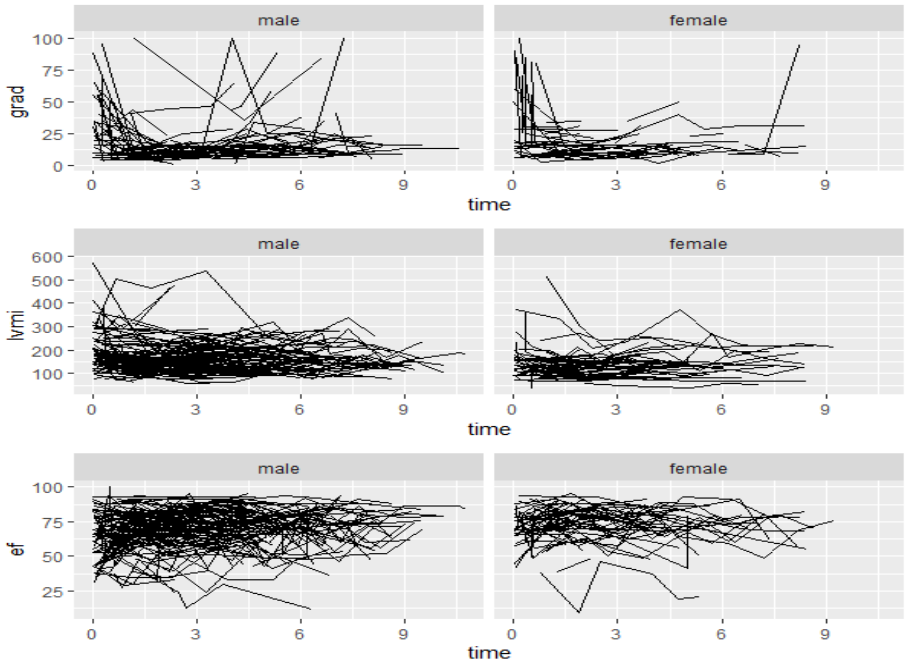


**Figure 2.** The Spaghetti Plot of longitudinal outcomes by gender covariate *sex.*

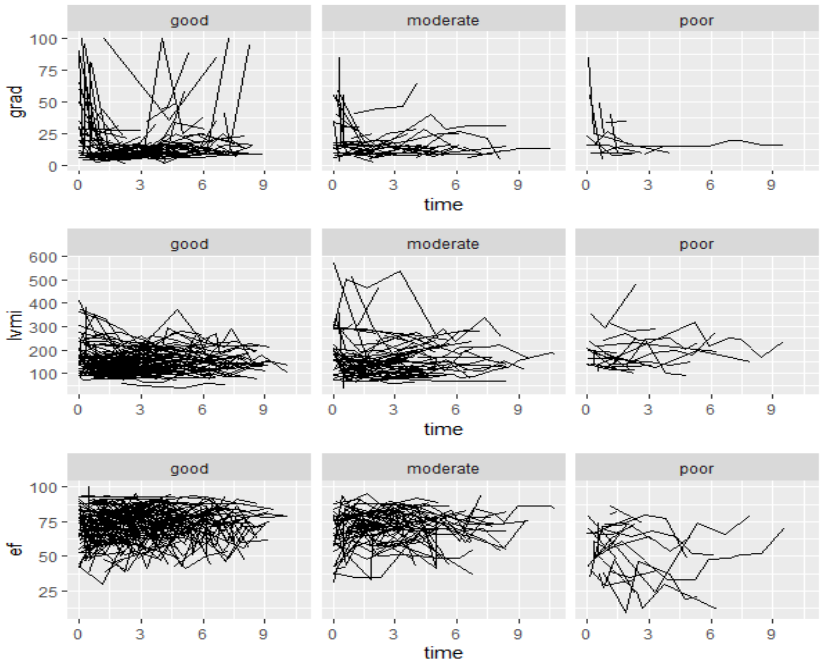


**Figure 3.** The Spaghetti Plot of longitudinal outcomes by preoperative left ventricular ejection fraction covariate *lv.*

We also examined the survival curves for the three covariates of type of implanted aortic prosthesis received, gender of patient and preoperative left ventricular ejection fraction, *hs*, *sex* and *lv*. From Figure 4 which shows the different survival curves estimated by gender, it can be observed that survival seemed to lower quickly for patients who received stentless valve replacement before flattening at 50% rate at less than two years after treatment. The patients with homograft valve replacement showed slower decrease in survival rate before flattening at aver 70% at less than two years after treatment. This information suggest the possibility of cure fraction for some patients who may not observe the failure event of death at the end of the follow-up period and or beyond.

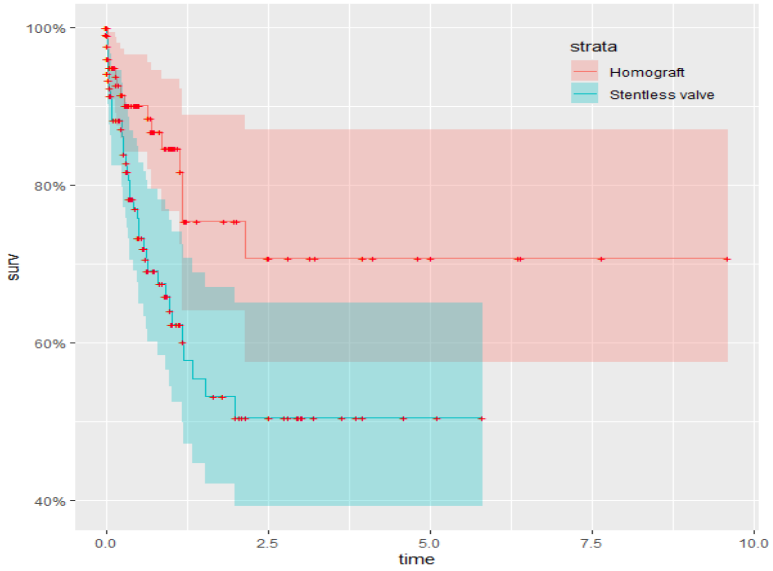


**Figure 4.** Survival estimates of patients according to treatment covariate *hs*.

The survival curve for male and female patients in Figure 5 showed that the survival rate lowered quickly for female patients than for male patients, but were at approximately the same flat level of 60% at about after one year at commencement of follow-up. Again the possibility of cure is observed for the dataset. Also Figure 6 showed that the survival rate was highest in patients with good preoperative left ventricular ejection fraction, then in patients with moderate preoperative left ventricular ejection fraction and lowest for those patients with poor preoperative left ventricular ejection fraction.

In investigating the survival time and censorship, association between these two variables may be explained by the longitudinal outcomes and as clinical state can be modelled on several covariates using longitudinal data, censoring also depends on these longitudinal outcomes (Gómez-Rubio, 2020), we examine the multivariate joint modelling of the three longitudinal outcomes and the survival time with possibility of cure proportion.

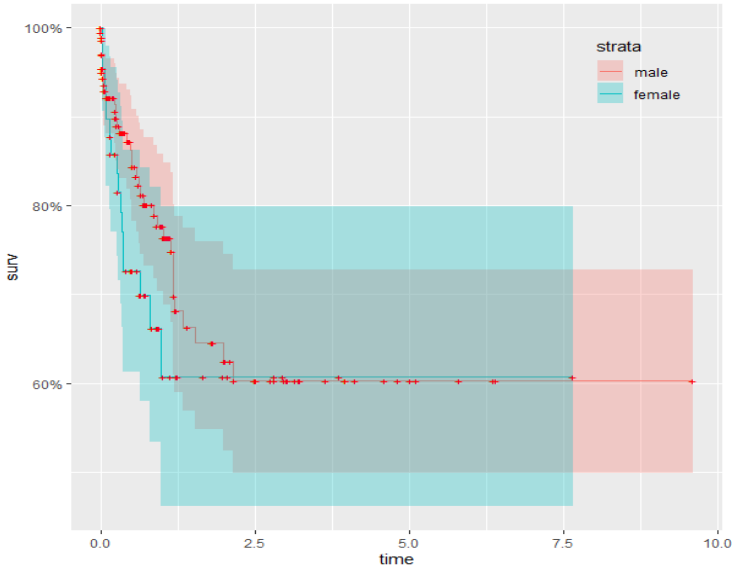


**Figure 5.** Survival estimates of patients according to gender covariate *sex*.

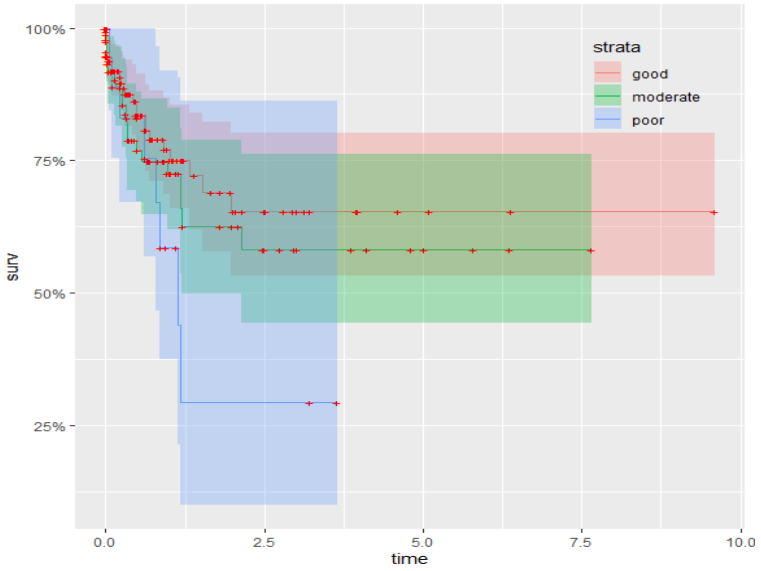


**Figure 6.** Survival estimates of patients according to preoperative left ventricular ejection fraction covariate *lv*.

## 3.2 Multivariate joint cure modelling of aortic valve replacement surgery data

Our approach here is to fit the multivariate joint model for the aortic valve replacement surgery data using the LGM framework as implemented with INLA by considering the possibilities of cure proportion in the survival component of the modelling. The modelling formulation as described in Section 2 is presented for the dataset thus.

Longitudinal component with linear trajectories:

$$\text{grad}_i(t) = (\beta_{10} + b_{i10}) + (b_{i11} + \beta_{1time})\text{time}_i + \beta_{1hs}\text{hs}_i + \beta_{1sex}\text{sex}_i + \beta_{1size}\text{size}_i + \beta_{1lv1}\text{lv}_i + \beta_{1lv2}\text{lv}_i + \varepsilon_{i1}(t) = \eta_{i1}(t) + \varepsilon_{i1}(t)$$

$$\text{lvmi}_i(t) = (\beta_{20} + b_{i20}) + (b_{i21} + \beta_{2time})\text{time}_i + \beta_{2hs}\text{hs}_i + \beta_{2sex}\text{sex}_i + \beta_{2size}\text{size}_i + \beta_{2lv1}\text{lv}_i + \beta_{2lv2}\text{lv}_i + \varepsilon_{i2}(t) = \eta_{i2}(t) + \varepsilon_{i2}(t)$$

$$\text{ef}_i(t) = (\beta_{30} + b_{i30}) + (b_{i31} + \beta_{3time})\text{time}_i + \beta_{3hs}\text{hs}_i + \beta_{3sex}\text{sex}_i + \beta_{3size}\text{size}_i + \beta_{3lv1}\text{lv}_i + \beta_{3lv2}\text{lv}_i + \varepsilon_{i3}(t) = \eta_{i3}(t) + \varepsilon_{i3}(t)$$

Longitudinal component with quadratic trajectories:

$$\text{grad}_i(t) = (\beta_{10} + b_{i10}) + (b_{i11} + \beta_{1time})\text{time}_i F_1(t) + \beta_{1hs}\text{hs}_i + \beta_{1sex}\text{sex}_i + \beta_{1size}\text{size}_i + \beta_{1lv1}\text{lv}_i + \beta_{1lv2}\text{lv}_i + \varepsilon_{i1}(t) = \eta_{i1}(t) + \varepsilon_{i1}(t)$$

$$\text{lvmi}_i(t) = (\beta_{20} + b_{i20}) + (b_{i21} + \beta_{2time})\text{time}_i F_1(t) + \beta_{2hs}\text{hs}_i + \beta_{2sex}\text{sex}_i + \beta_{2size}\text{size}_i + \beta_{2lv1}\text{lv}_i + \beta_{2lv2}\text{lv}_i + \varepsilon_{i2}(t) = \eta_{i2}(t) + \varepsilon_{i2}(t)$$

$$\text{ef}_i(t) = (\beta_{30} + b_{i30}) + (b_{i31} + \beta_{3time})\text{time}_i F_1(t) + \beta_{3hs}\text{hs}_i + \beta_{3sex}\text{sex}_i + \beta_{3size}\text{size}_i + \beta_{3lv1}\text{lv}_i + \beta_{3lv2}\text{lv}_i + \varepsilon_{i3}(t) = \eta_{i3}(t) + \varepsilon_{i3}(t)$$

Longitudinal component with spline trajectories:

$$\text{grad}_i(t) = (\beta_{10} + b_{i10})F_2(t) + (b_{i11} + \beta_{1time})\text{time}_i F_3(t) + \beta_{1hs}\text{hs}_i + \beta_{1sex}\text{sex}_i + \beta_{1size}\text{size}_i + \beta_{1lv1}\text{lv}_i + \beta_{1lv2}\text{lv}_i + \varepsilon_{i1}(t) = \eta_{i1}(t) + \varepsilon_{i1}(t)$$

$$\text{lvmi}_i(t) = (\beta_{20} + b_{i20})F_2(t) + (b_{i21} + \beta_{2time})\text{time}_i F_3(t) + \beta_{2hs}\text{hs}_i + \beta_{2sex}\text{sex}_i + \beta_{2size}\text{size}_i + \beta_{2lv1}\text{lv}_i + \beta_{2lv2}\text{lv}_i + \varepsilon_{i2}(t) = \eta_{i2}(t) + \varepsilon_{i2}(t)$$

$$\text{ef}_i(t) = (\beta_{30} + b_{i30})F_2(t) + (b_{i31} + \beta_{3time})\text{time}_i F_3(t) + \beta_{3hs}\text{hs}_i + \beta_{3sex}\text{sex}_i + \beta_{3size}\text{size}_i + \beta_{3lv1}\text{lv}_i + \beta_{3lv2}\text{lv}_i + \varepsilon_{i3}(t) = \eta_{i3}(t) + \varepsilon_{i3}(t)$$

Latency model component:

$$h_i(t\,|h_0) = (\lambda\alpha t^{\alpha-1})\exp\{\gamma_{\text{grads}}(\eta_{i1}(t)) + \gamma_{\text{lvmis}}(\eta_{i2}(t)) + \gamma_{\text{efs}}(\eta_{i3}(t)) + (\beta_{4hs}\text{hs}_i + \beta_{4sex}\text{sex}_i + \beta_{4size}\text{size}_i + \beta_{4lv1}\text{lv}_i + \beta_{4lv2}\text{lv}_i)\}$$

Incidence model component:

$$\text{logit}[\pi_i] = \beta_{50} + \beta_{5hs}\text{hs}_i + \beta_{5sex}\text{sex}_i + \beta_{5size}\text{size}_i + \beta_{5lv1}\text{lv}_i + \beta_{5lv2}\text{lv}_i$$

where $\varepsilon_{ij}(t),\ j = 1,2,3$ are independent Gaussian measurement errors for the longitudinal outcomes, $F_1(t)$ is a quadratic function and $F_2(t)$ and $F_3(t)$ are natural cubic spline basis functions with internal knots at 2 years. For priors specification, as noted earlier, we assume a multivariate Gaussian prior for the latent field $\boldsymbol{\chi}$ with precision matrix $\boldsymbol{Q}(\boldsymbol{\theta})$ conditioned on $\boldsymbol{\theta}$, which we also assume prior distributions $p(\boldsymbol{\theta})$ for which all the regression coefficients and the Weibull log(λ) scale parameters follow a vague normal distribution centred at zero ($\mathcal{N}(0{,}1000)$) while the shape parameter, α, is assumed to follow the penalised complexity prior PC(5). The inverse-Wishart prior distribution is assumed for the covariance matrix of the random effects and Gaussian priors for all the fixed effects.

The results of the multivariate joint modelling of the effects of different heart valves on valve gradient (*grad*), left ventricular mass index (*lvmi*) and ejection fraction (*ef*) and the risk of death after aortic valve replacement surgery implemented using R packages INLA and INLAjoint, is herein presented. Firstly, we fitted the multivariate joint cure modelling with the three longitudinal trajectories and three association specifications on the aortic valve replacement surgery data and compare the model fits using marginal log-likelihood, DIC and WAIC as given in Table 1, which includes the computation times for each model. From the table, it is seen that the spline-CS model was the best fit with the lowest marginal log-likelihood, DIC and WAIC. The linear-CS model followed after spline-CS model and the computation times showed that the models with CS specification ran quickest than the others, irrespective of the longitudinal trajectory used. In what follows we considered the parameter estimates for the CS specification in each longitudinal trajectory, linear, quadratic and spline.

**Table 1.** Comparisons of longitudinal trajectories and association specifications for the of aortic valve replacement surgery dataset

| trajectory | association | log-lik | DIC | WAIC | Comp time (seconds) |
|---|---|---|---|---|---|
| linear | CV | -28966.32 | 24634.46 | 24162.27 | 3759.84 |
| linear | CS | -18378.91 | 10782.04 | 10383.83 | 442.52 |
| linear | SRE | -18395.04 | 10870.84 | 10421.50 | 411.66 |
| quadratic | CV | -19502.73 | 11774.21 | 11321.52 | 574.11 |
| quadratic | CS | -18440.06 | 11001.98 | 10526.94 | 237.89 |
| quadratic | SRE | -18462.96 | 11069.63 | 10923.14 | 1035.21 |
| spline | CV | -21093.16 | 15500.44 | 15027.05 | 2448.63 |
| spline | CS | -18369.21 | 10704.01 | 10316.15 | 510.61 |
| spline | SRE | -18637.33 | 11880.84 | 11481.90 | 3241.64 |

Table 2A and Table 2B shows the posterior mean and standard deviation for the multivariate joint modelling including cure proportion of the aortic valve replacement surgery data for linear, spline and quadratic longitudinal trajectories. The outputs include the longitudinal component, the latency and incidence survival parts, as well as the association parameters. The parameter estimates are similar for the three models. The three models showed that the significant predictors for valve

gradient were gender and preoperative left ventricular ejection fraction, for both left ventricular mass index and ejection fraction, the significant predictors were the type of implanted aortic prosthesis, gender, size of valve and preoperative left ventricular ejection fraction.

**Table 2A.** Posterior mean and standard deviation of aortic valve replacement surgery data output for linear, spline and quadratic trajectories

| | Linear | | Spline | | Quadratic | |
|---|---|---|---|---|---|---|
| *Fixed effects* | mean | sd | mean | sd | mean | sd |
| *grad* | | | | | | |
| $\beta_{10}$ | 1.81080 | 2.40770 | 2.30320 | 2.40160 | 1.47580 | 2.42780 |
| $\beta_{1time}$ | -0.02560 | 0.29740 | -1.96370 | 1.97310 | -0.02150 | 0.03760 |
| $\beta_{1hs}$ | 0.52360 | 1.37680 | 0.29250 | 1.30910 | 1.54430 | 1.51610 |
| $\beta_{1sex}$ | 3.49240 | 1.33580 | 3.68830 | 1.29040 | 3.45750 | 1.47730 |
| $\beta_{1size}$ | 0.63110 | 0.13410 | 0.63140 | 0.11520 | 0.64940 | 0.12640 |
| $\beta_{1lv1}$ | -1.22830 | 1.35800 | -1.17300 | 1.30870 | -1.19770 | 1.49970 |
| $\beta_{1lv2}$ | 1.88340 | 1.84470 | 1.81160 | 1.80470 | 1.43300 | 1.91950 |
| $\sigma_{e1}$ | 291.41490 | 30.72360 | 303.22370 | 15.94920 | 266.8592 | 16.28620 |
| *lvmi* | | | | | | |
| $\beta_{20}$ | 0.52800 | 2.48920 | 0.59390 | 2.49110 | 0.49340 | 2.48910 |
| $\beta_{2time}$ | 0.02970 | 0.82500 | -0.00780 | 2.26570 | -0.04530 | 0.17220 |
| $\beta_{2hs}$ | -2.30440 | 2.31330 | -1.85840 | 2.35470 | -2.45380 | 2.31080 |
| $\beta_{2sex}$ | -2.08050 | 2.31540 | -1.68350 | 2.35760 | -2.28300 | 2.31020 |
| $\beta_{2size}$ | 6.56040 | 0.20370 | 6.52220 | 0.19050 | 6.63040 | 0.20190 |
| $\beta_{2lv1}$ | -0.04190 | 2.31100 | -0.25680 | 2.35290 | -0.31140 | 2.30810 |
| $\beta_{2lv2}$ | 1.12580 | 2.41700 | 0.79080 | 2.43780 | 1.46370 | 2.40810 |
| $\sigma_{e2}$ | 1774.0180 | 130.6978 | 1608.7339 | 84.38370 | 1982.827 | 113.2824 |
| *ef* | | | | | | |
| $\beta_{30}$ | 7.04500 | 2.39550 | 6.12420 | 2.40710 | 8.40420 | 2.38340 |
| $\beta_{3time}$ | 0.61290 | 0.29490 | 2.92200 | 2.12550 | 0.06880 | 0.03660 |
| $\beta_{3hs}$ | -7.23330 | 1.29020 | -7.32950 | 1.34660 | -7.85900 | 1.22510 |
| $\beta_{3sex}$ | 5.18530 | 1.27800 | 4.88770 | 1.34330 | 6.14730 | 1.21020 |
| $\beta_{3size}$ | 2.55470 | 0.12340 | 2.66720 | 0.11880 | 2.54880 | 0.11370 |
| $\beta_{3lv1}$ | -1.39040 | 1.27680 | -1.76150 | 1.33480 | -1.85230 | 1.20830 |
| $\beta_{3lv2}$ | -6.32040 | 1.71170 | -5.97150 | 1.78160 | -6.89550 | 1.62160 |
| $\sigma_{e3}$ | 117.3553 | 9.22890 | 114.0684 | 5.74370 | 132.6199 | 7.50720 |
| *Random effects* | | | | | | |
| $\sigma^2_{b10}$ | 11.56870 | 98.39430 | 12.12570 | 11.85350 | 0.07930 | 0.12970 |
| $\sigma^2_{b11}$ | 5272.3066 | 100057.0 | 2995.1126 | 1038.561 | 7.49290 | 9.47890 |
| $\sigma^2_{b20}$ | 827.5162 | 18884.34 | 141.1984 | 54.8680 | 0.19480 | 0.19040 |
| $\sigma^2_{b21}$ | 134.0140 | 3087.596 | 0.2164 | 0.1217 | 0.37120 | 0.88640 |
| $\sigma^2_{b30}$ | 2.68520 | 13.61280 | 0.20270 | 0.12160 | 0.29660 | 1.22600 |
| $\sigma^2_{b31}$ | 0.49120 | 0.75410 | 0.23480 | 0.13130 | 0.24300 | 0.16820 |

The valve gradient was higher in female patients with male reference, decreased in patients with moderate preoperative left ventricular ejection fraction and increased in patients with poor preoperative left ventricular ejection fraction both with good preoperative left ventricular ejection fraction as reference. The left ventricular mass index with significant predictors as type of implanted aortic prosthesis, gender and size of valve was lower in female patients and patients treated with stentless valve. The ejection fraction had type of implanted aortic prosthesis, gender, size of valve and preoperative left ventricular ejection fraction as significant predictors in the three models. However, we see that the time effect in the spline model was significant to capture the longitudinal profile of ejection fraction. The ejection fraction decreased in patients with moderate and poor preoperative left ventricular ejection fraction against those with good preoperative left ventricular ejection fraction.

From Table 2B, the type of implanted aortic prosthesis, gender, size of valve and preoperative left ventricular ejection fraction were also significant in the conditional failure time latency model, as evidenced in the survival curves plots in Section 3.1.

**Table 2B.** Posterior mean and standard deviation of aortic valve replacement surgery data output for linear, spline and quadratic trajectories (continuation)

| | Linear | | Spline | | Quadratic | |
|---|---|---|---|---|---|---|
| | mean | sd | mean | sd | mean | sd |
| *covariance* | | | | | | |
| $cov_{b10,b11}$ | 46.67060 | 1650.229 | 127.36600 | 96.95670 | 0.32260 | 0.77180 |
| $cov_{b10,b20}$ | -4.31680 | 730.1053 | 14.10150 | 16.19890 | -0.02750 | 0.09680 |
| $cov_{b10,b21}$ | -2.53490 | 274.7368 | -0.39150 | 0.84510 | 0.03130 | 0.29660 |
| $cov_{b10,b30}$ | 1.58300 | 29.83760 | 0.47300 | 0.49390 | 0.02110 | 0.21970 |
| $cov_{b10,b31}$ | -0.34530 | 4.38210 | -0.43090 | 0.75690 | -0.00070 | 0.07860 |
| $cov_{b11,b20}$ | -1957.1171 | 42950.23 | -214.27530 | 138.3266 | -0.85930 | 1.16730 |
| $cov_{b11,b21}$ | -794.42290 | 17327.15 | -1.78480 | 10.04970 | -0.14240 | 2.11750 |
| $cov_{b11,b30}$ | -51.23850 | 673.0084 | 6.44130 | 7.79560 | 0.17330 | 2.09330 |
| $cov_{b11,b31}$ | 7.37890 | 172.0917 | -10.65570 | 10.18110 | 0.08390 | 0.99360 |
| $cov_{b20,b21}$ | 324.51240 | 7478.755 | -1.01510 | 1.98350 | 0.02420 | 0.29720 |
| $cov_{b20,b30}$ | 21.18590 | 300.9063 | 0.54790 | 1.86490 | -0.02890 | 0.21330 |
| $cov_{b20,b31}$ | -3.74840 | 72.22530 | 0.82960 | 2.39560 | -0.02880 | 0.13400 |
| $cov_{b21,b30}$ | 8.34740 | 111.3181 | -0.06750 | 0.06270 | -0.03210 | 0.67160 |
| $cov_{b21,b31}$ | -1.50990 | 28.25780 | -0.01810 | 0.08720 | 0.00860 | 0.20550 |
| $cov_{b30,b31}$ | -0.53140 | 2.02600 | 0.01450 | 0.06340 | 0.01550 | 0.20890 |
| *Latency estmates* | | | | | | |
| $\alpha$ | 0.67380 | 0.07880 | 0.79550 | 0.03300 | 0.68980 | 0.08440 |
| $\lambda$ | 1.16960 | 2.35770 | 1.04930 | 2.05140 | 3.56830 | 7.17300 |
| $\beta_{4hs}$ | 1.05270 | 0.36040 | 1.01650 | 0.35250 | 1.14750 | 0.36620 |
| $\beta_{4sex}$ | 0.37480 | 0.32910 | 0.34300 | 0.31560 | 0.23530 | 0.32200 |
| $\beta_{4size}$ | -0.04370 | 0.06240 | -0.06190 | 0.06140 | -0.09090 | 0.06250 |
| $\beta_{4lv1}$ | 0.10690 | 0.31200 | 0.02910 | 0.29930 | 0.21920 | 0.30720 |
| $\beta_{4lv2}$ | 0.26870 | 0.42950 | 0.16100 | 0.41000 | 0.25330 | 0.41880 |

| | | | | | | |
|---|---|---|---|---|---|---|
| *Incidence estimates* | | | | | | |
| $\beta_{50}$ | 0.14460 | 1.69820 | 0.14460 | 1.69820 | 0.14460 | 1.69820 |
| $\beta_{5hs}$ | -0.17680 | 0.33870 | -0.17680 | 0.33870 | -0.17680 | 0.33870 |
| $\beta_{5sex}$ | -0.50800 | 0.31040 | -0.50800 | 0.31040 | -0.50800 | 0.31040 |
| $\beta_{5size}$ | -0.01210 | 0.07220 | -0.01210 | 0.07220 | -0.01210 | 0.07220 |
| $\beta_{5lv1}$ | 0.04730 | 0.28090 | 0.04730 | 0.28090 | 0.04730 | 0.28090 |
| $\beta_{5lv2}$ | -0.04570 | 0.47220 | -0.04570 | 0.47220 | -0.04570 | 0.47220 |
| *Association parameters* | | | | | | |
| $\gamma_{grad\_S}$ | 0.89560 | 0.83530 | -0.83910 | 0.59860 | 0.11300 | 1.10870 |
| $\gamma_{lvmi\_S}$ | 0.00700 | 0.06850 | -0.03720 | 0.05240 | -0.00300 | 0.11640 |
| $\gamma_{ef\_S}$ | -0.20070 | 0.38620 | 0.29350 | 0.22160 | -1.44490 | 0.53140 |

For the incidence model, the significant predictors were type of implanted aortic prosthesis and gender, where the cure variable is has a negative log-odds coefficients for patients treated with stentless valve and female patients. The association parameter estimates from the three models differ for the three longitudinal outcomes with risk of survival. The linear and spline trajectories showed significant association of the survival component with the longitudinal trajectory of valve gradient, while all three models showed significant association of survival component with the longitudinal ejection fraction variable. However, there were differences in the sign of the posterior mean values for the association parameters for valve gradient and ejection fraction in the linear and spline, and quadratic and spline models respectively. The case of negative association parameter indicates that higher values of the longitudinal outcome implies that there was a reduction in the probability in the risk of the event. The spline model then, seemed to give the best situation of the joint modelling of the three longitudinal outcomes (grad, lvmi and ef) with survival component including cure proportion, since the association parameter values had signs indicating the direction of the longitudinal outcomes in relation to the probability of survival, as was also observed in the descriptives of the dataset done in Section 3.1.

We now turn to the discussion on the cure proportion from the model results, we particularly took the spline model as the best fit model for the dataset and examined the result for the cure proportions. The full conditional distribution of latent incidence variable $Z$ gave a predicted cure proportion of 36.3281%. Table 3 shows the posterior mean, standard deviation and 95% credible interval of the posterior distribution of the cure proportion comprising patients in ten groups formed by the combinations of the covariate factor levels, for the factors *hs* (type of implanted aortic prosthesis) *sex* (male or female) and *lv* (state of preoperative left ventricular ejection fraction). The highest cure proportion estimates was in the groups of men treated with homograft valve, while the lowest values are in the groups of women treated with stentless valve.

**Table 3.** Posterior mean, standard deviation, and 95% credible interval of the cure proportion for covariates' levels combinations

| *hs* | *sex* | *lv* | *mean* | *sd* | *Lw 95% CI* | *Up 95% CI* |
|---|---|---|---|---|---|---|
| Homograft | male | good | 0.306 | 0.00315 | 0.303 | 0.309 |
| Homograft | male | moderate | 0.306 | 0.00300 | 0.303 | 0.309 |
| Homograft | male | poor | 0.303 | NA | 0.303 | 0.303 |
| Homograft | female | good | 0.212 | 0.00192 | 0.21 | 0.214 |
| Homograft | female | moderate | 0.211 | 0.00330 | 0.212 | 0.214 |

| | | | | | | |
|---|---|---|---|---|---|---|
| Stentless | male | good | 0.263 | 0.00559 | 0.258 | 0.265 |
| Stentless | male | moderate | 0.263 | 0.00503 | 0.26 | 0.266 |
| Stentless | male | poor | 0.263 | 0.00535 | 0.26 | 0.265 |
| Stentless | female | good | 0.178 | 0.00267 | 0.176 | 0.178 |
| Stentless | female | moderate | 0.178 | 0.00000 | 0.178 | 0.178 |

## 4. Conclusions

This paper presented the modelling of multivariate longitudinal outcomes and mixture cure survival under shared random effect using latent Gaussian modelling approach, which involves the deterministic approximate Bayesian inference of Laplace approximation in evaluating the posterior distribution of the resulting Bayesian modelling and hence how the integrated Laplace approximation (INLA) introduced by Rue *et al.*, (2009) can be used to evaluate its posteriors. For the longitudinal outcomes a linear, quadratic and spline specifications were studied in capturing the complex evolutions and the survival cure component was based on the specifications by Lázaro *et al.*, (2020), in which latent indicators in the inferential process for classifying patients in the cured and uncured groups by a latent indicator variable was introduced. The multivariate joint cure modelling approach involved expressing the joint model as a hierarchical structure fitting the structure of latent Gaussian models under the Bayesian paradigm and then using the INLA to evaluate the marginal posterior distributions for the joint multivariate models.

The multivariate joint cure modelling approach was applied to the aortic valve replacement surgery data to study the effects of different heart valves on valve gradient (grad), left ventricular mass index (*lvmi*) and ejection fraction (*ef*) and the risk of death after aortic valve replacement surgery. We fitted the multivariate joint cure modelling with the three longitudinal trajectories and three association specifications on the aortic valve replacement surgery data and compared the model fits using marginal log-likelihood, DIC and WAIC and saw that the spline trajectory with current slope association was the best fit with the lowest marginal log-likelihood, DIC and WAIC. The spline model gave the best situation of the joint modelling of the three longitudinal outcomes (*grad*, *lvmi* and *ef*) with survival component including cure proportion, and the signs of the association parameter values indicated the direction of the longitudinal outcomes in relation to the probability of survival.

The full conditional distribution of latent incidence variable Z gave a predicted cure proportion of 36.33% and it was concluded that the type of treatment valve received and gender of patients were clinically significant in the proportion of cure as were in the case of latency and longitudinal outcomes processes of the aortic valve replacement surgery process. The survival profiles of the patients in the uncured group were very different and the worst survival expectations were found in the factor-level combinations of female patients who received stentless valve for replacement, irrespective of the patient's preoperative condition of the left ventricular ejection fraction. However, female patients who received homograft valve for replacement had higher survival functions as do male patients. Hence, the probability of cure was seen to be a function of the type of implanted aortic prosthesis received by patients and gender of patients.

The merit of this approach is that apart from capturing the nonlinear trajectory of the longitudinal outcomes, the association between the longitudinal component and survival components which included cure fractions was also estimated. This study adds to the body

of work on the application of the deterministic inference strategy, INLA, to other joint modelling development as well as other modelling approaches where they can be expressed as latent Gaussian model and affords the ease of computation even with large datasets with less powerful computers as seen in this study. The issue of missing values and observation of short credible intervals reported in the predictive distribution of the cure proportion raises areas of further study with INLA for joint model in the context of this study.

## Funding

This research did not receive any specific grant from funding agencies in the public, commercial, or not-for-profit sectors.

## Conflicts of Interest

The authors declare no conflict of interest.

## Author Contributions

**Conceptualization:** EKONG, A. H.; OLAYIWOLA, M. O. **Data curation:** EKONG, A. H. **Formal analysis:** EKONG, A. H. **Investigation:** EKONG, A. H. **Methodology:** EKONG, A. H. **Project administration:** EKONG, A. H. **Software:** EKONG, A. H. **Resources:** EKONG, A. H. **Supervision:** OLAYIWOLA, M. O.; OSINUGA, I. A.; DAWODU, G. A. **Validation:** **Visualization:** EKONG, A. H. **Writing - original draft:** EKONG, A. H. **Writing - review and editing:** EKONG, A. H.

## References

1. Alafchi, B., Mahjub, H., Tapak, L., Roshanaei,G. & Amirzargar, M.A.Two-Stage Joint Model for Multivariate Longitudinal and Multistate Processes, with Application to Renal Transplantation Data. *Journal of Probability and Statistics* Volume 2021, Article ID 6641602, 10 (20210 https://doi.org/10.1155/2021/6641602
2. Alsefri, M., Sudell, M., García-Fiñana, M., & Kolamunnage-Dona, R. Bayesian joint modelling of longitudinal and time to event data: a methodological review. *BMC Medical Research Methodology*, **20**(1), 94 (2020). https://doi.org/10.1186/s12874-020-00976-2
3. Alvares, D., van Niekerk, J., Krainski, E. T., Rue, H. & Rustand, D. Bayesian survival analysis with INLA. *Statistics in Medicine*, 1–36 (2024). DOI: 10.1002/sim.10160
4. Blangiardo M. & Cameletti M. *Spatial and Spatio-temporal Bayesian Models with R –INLA*. John Wiley & Sons, Chichester, (2015). DOI:10.1002/9781118950203
5. Chen M.H, Ibrahim J.G, & Sinha D. A new joint model for longitudinal and survival data with a cure fraction. *J Multivar Anal* **91**(1):18–34 (2004). https://doi.org/10.1016/j.jmva.2004.04.005
6. Chi, Y. Y., & Ibrahim, J. G. Bayesian approaches to joint longitudinal and survival models accommodating both zero and nonzero cure fractions. Statistica Sinica, **17** (2), pp. 445–462 (2007).
7. Cox, D. R. Regression Models and Life-Tables. Journal of the Royal Statistical Society: Series B (Methodological), **34** (2), pp. 187–202 (1972). https://doi.org/10.1111/j.2517-6161.1972.tb00899.x

8. Ekong, A., Olayiwola, M., Dawodu, A., & Osinuga, A. Latent Gaussian Approach to Joint Modelling of Longitudinal and Mixture Cure Outcomes. *Computational Journal of Mathematical and Statistical Sciences*, **4**(1), 72-95 (2025). http://doi: 10.21608/cjmss.2024.303748.1061
9. Gómez-Rubio, V. *Bayesian Inference with INLA*. Chapman and Hall/CRC. (2020). https://doi.org/10.1201/9781315175584
10. He, B., & Luo, S. Joint modeling of multivariate longitudinal measurements and survival data with applications to Parkinson's disease. *Statistical methods in medical research*, **25**(4), 1346–1358 (2016). https://doi.org/10.1177/0962280213480877
11. Hickey, G. L., Philipson, P., Jorgensen, A., & Kolamunnage-Dona, R. Joint Models of Longitudinal and Time-to-Event Data with More Than One Event Time Outcome: A Review. *The International Journal of Biostatistics*, **14**(1) (2018a). https://doi.org/10.1515/ijb-2017-0047
12. Hickey, G. L., Philipson, P., Jorgensen, A., & Kolamunnage-Dona, R. JoineRML: A joint model and software package for time-to-event and multivariate longitudinal outcomes. *BMC Medical Research Methodology*, **18**(1), 1–14 (2018b). https://doi.org/10.1186/s12874-018-0502-1
13. Kalbfleisch, J. D., & Prentice, R. L. The Statistical Analysis of Failure Time Data. Wiley. (2002). https://doi.org/10.1002/9781118032985
14. Lázaro, E., Armero, C., & Gómez-Rubio, V. Approximate Bayesian inference for mixture cure models. *Test*, **29**(3), 750–767 (2020). https://doi.org/10.1007/s11749-019-00679-x
15. Li, N., Liu, Y., Li, S., Elashoff, R. M., & Li, G. A flexible joint model for multiple longitudinal biomarkers and a time-to-event outcome: With applications to dynamic prediction using highly correlated biomarkers. *Biometrical journal. Biometrische Zeitschrift*, **63**(8), 1575–1586 (2021). https://doi.org/10.1002/bimj.202000085
16. Lim, E., Ali, A., Theodorou, P., Sousa, I., Ashrafian, H., Chamageorgakis, T., Duncan, A., Henein, M., Diggle, P., & Pepper, J. Longitudinal study of the profile and predictors of left ventricular mass regression after stentless aortic valve replacement. *The Annals of thoracic surgery*, **85**(6), 2026–2029 (2008). https://doi.org/10.1016/j.athoracsur.2008.02.023
17. Martins, R., Silva, G. L., & Andreozzi, V. Joint analysis of longitudinal and survival AIDS data with a spatial fraction of long-term survivors: A Bayesian approach. *Biometrical Journal*, **59**(6), 1166–1183 (2017). https://doi.org/10.1002/bimj.201600159
18. Mayer, F. P., Sant'Ana, R., & Ribeiro Junior, P. J. MODELAGEM DA ESTRUTURA TEMPORAL DE CAPTURAS INCIDENTAIS EM PESCARIAS COMERCIAIS ATRAVÉS DE MODELOS HIERÁRQUICOS BAYESIANOS. *Brazilian Journal of Biometrics*, **37**(4), 446–466 (2019). https://doi.org/10.28951/rbb.v37i4.417
19. Medina-Olivares, V., Calabrese, R., Crook, J., & Lindgren, F. Joint models for longitudinal and discrete survival data in credit scoring. *European Journal of Operational Research*, **307**(3), 1457–1473 (2023a). https://doi.org/10.1016/J.EJOR.2022.10.022
20. Medina-Olivares, V., Lindgren, F., Calabrese, R., & Crook, J. Joint models of multivariate longitudinal outcomes and discrete survival data with INLA: An application to credit repayment behaviour. *European Journal of Operational Research*, **310**(2), 860–873 (2023b). https://doi.org/10.1016/j.ejor.2023.03.012
21. Murray, J. & Philipson, P. A fast approximate EM algorithm for joint models of survival and multivariate longitudinal data. *Computational Statistics and Data Analysis* **170**, 107438 (2020). https://doi.org/10.1016/j.csda.2022.107438

22. Oliveira, M. H., Abosamak, M. F., Michael Henry, B., W Benoit, S., Lippi, G., & Previdelli, I. Longitudinal serum chloride as a marker for poor prognosis in severely ill COVID-19 patients: A joint model approach. *Brazilian Journal of Biometrics*, **42**(1), 88–99 (2024). https://doi.org/10.28951/bjb.v42i1.670
23. Opitz T. Latent Gaussian modeling and INLA: A review with focus on space-time applications. *Journal of the French Statistical Society* **158**(3), 62-85 (2017). https://www.numdam.org/item/JSFS_2017__158_3_62_0/
24. Peng, Y., & Taylor, J. M. G. Cure Models. *In Handbook of Survival Analysis*, 113–134 (2014). https://doi.org/10.1201/b16248
25. Philipson, P., Hickey, G. L., Crowther, M. J. & Kolamunnage-Dona, R. Faster Monte Carlo estimation of joint models for time-to-event and multivariate longitudinal data. *Computational Statistics and Data Analysis* **151**, 107010 (2020). https://doi.org/10.1016/j.csda.2020.107010
26. Rue, H., & Held, L. Gaussian Markov Random Fields. Chapman and Hall/CRC. (2005). https://doi.org/10.1201/9780203492024
27. Rue, H., Martino, S., & Chopin, N. Approximate Bayesian inference for latent Gaussian models by using integrated nested Laplace approximations. *Journal of the Royal Statistical Society. Series B: Statistical Methodology*, **71**(2), 319–392 (2009) https://doi.org/10.1111/J.1467-9868.2008.00700.X
28. Rustand, D., van Niekerk, J., Rue, H., Tournigand, C., Rondeau, V., & Briollais, L. Bayesian estimation of two-part joint models for a longitudinal semicontinuous biomarker and a terminal event with INLA: Interests for cancer clinical trial evaluation. *Biometrical Journal*, **65**(4) (2023). https://doi.org/10.1002/bimj.202100322
29. Rustand, D., van Niekerk, J., Krainski, E. T., Rue, H., & Proust-Lima, C. Fast and flexible inference for joint models of multivariate longitudinal and survival data using integrated nested Laplace approximations. *Biostatistics*, 2024, **25** (2) pp. 429–448 (2024a). https://doi.org/10.1093/biostatistics/kxad019
30. Rustand, D., van Niekerk, J., Krainski, E. T., & Rue, H. Joint Modeling of Multivariate Longitudinal and Survival Outcomes with the R package INLAjoint. (2024b) https://doi.org/10.48550/arXiv.2402.08335
31. Tsiatis, A. A., & Davidian, M. Joint modelling of longitudinal and time-to-event data: An overview. *Statistica Sinica*, **14**(3), 809–834 (2004). https://www3.stat.sinica.edu.tw/statistica/j14n3/j14n39/j14n39.html
32. van Niekerk, J., Bakka, H., & Rue, H. Joint models as latent Gaussian models - not reinventing the wheel. (2019). http://arxiv.org/abs/1901.09365
33. van Niekerk, J., Bakka, H., & Rue, H. Competing risks joint models using R-INLA. *Statistical Modelling*, **21**(1–2), 56–71 (2021). https://doi.org/10.1177/1471082X20913654
34. Yu, M., Taylor, J. M. G., & Sandler, H. M. Individual Prediction in Prostate Cancer Studies Using a Joint Longitudinal Survival–Cure Model. Journal of the American Statistical Association, **103**(481), pp. 178–187 (2008). https://doi.org/10.1198/016214507000000400